HEiDi

Hot Single Crystal Diffractometer
for Structure Analysis with Neutrons

Martin Meven

RWTH Aachen University, Institute of Crystallography (IfK) and
Forschungszentrum Jülich, Jülich Centre for Neutron Science (JCNS)
at Heinz Maier-Leibnitz Zentrum (MLZ)

Contents

1   Introduction

Many properties of solid matter like their mechanical, thermal, optical, electrical and magnetic properties depend strongly on their atomic structure. Therefore, a good understanding of the physical properties needs not only the knowledge about the particles inside (atoms, ions, molecules) but also about their spatial arrangement. For most cases diffraction is *the* tool to answer questions about the atomic and/or magnetic structure of a system. Beyond this, neutron diffraction allows to answer questions where other techniques fail.

2   Crystallographic Basics

In the ideal case a complete solid matter consists of small identical units (same content, same size, same orientation like sugar pieces in a box). These units are called unit cells. A solid matter made of these cells is called a single crystal. The shape of a unit cell is equivalent to a parallelepiped that is defined by its base vectors $\mathbf{a_1}$, $\mathbf{a_2}$ und $\mathbf{a_3}$ and that can be described by its lattice constants a, b, c; α, β and γ (pic. 1). Typical lengths of the edges of such cells are between a few and a few ten Angstrom ($1\text{Å}=10^{-10}$ m). The combination of various restrictions of the lattice constants between $a \neq b \neq c$; $\alpha \neq \beta \neq \gamma \neq 90°$ (triclinic) and $a = b = c$; $\alpha = \beta = \gamma = 90°$ (cubic) yields seven crystal systems. The request to choose the system with the highest symmetry to describe the crystal structure yields fourteen Bravais lattices, seven primitive and seven centered lattices.
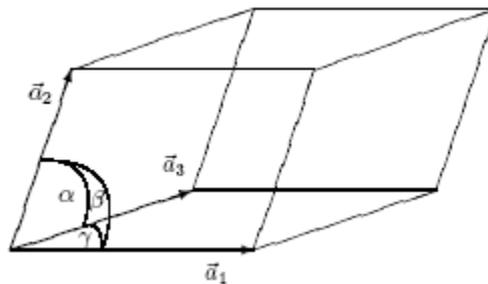
Fig. 1: Unit cell with $|\mathbf{a_1}|=a$, $|\mathbf{a_2}|=b$, $|\mathbf{a_3}|=c$, α, β, γ

Each unit cell contains one or more particles i. The referring atomic positions $\mathbf{x_i}=x_i*\mathbf{a_1} + y_i*\mathbf{a_2} + z_i*\mathbf{a_3}$ are described in relative coordinates $0 \leq x_i$; y_i; $z_i < 1$. The application of different symmetry operations (mirrors, rotations, glide mirrors, screw axes) on the atoms in one cell yield the 230 different space groups (see [1]).

The description of a crystal using identical unit cells allows the representation as a three dimensional lattice network. Each lattice point can be described as the lattice vector $\mathbf{t} = u*\mathbf{a_1} + v*\mathbf{a_2} + w*\mathbf{a_3}$; $u, v, w \in \mathbf{Z}$. From this picture we get the central word for diffraction in crystals; the *lattice plane* or *diffraction plane*. The orientations of these planes in the crystal are described by the so called *Miller indices* h, k and l with $h, k, l \in \mathbf{Z}$ (see pic. 2). The reciprocal base vectors $\mathbf{a^*_1}$, $\mathbf{a^*_2}$, $\mathbf{a^*_3}$ create the reciprocal space with: $\mathbf{a^*_i} * \mathbf{a_j} = \delta_{ij}$ with $\delta_{ij}=1$ for $i=j$ and $\delta_{ij}=0$ for $i \neq j$. Each point $\mathbf{Q}=h*\mathbf{a^*_1} + k*\mathbf{a^*_2} + l*\mathbf{a^*_3}$ represents the normal vector of

a (*hkl*) Plane. Each plane cuts the crystal lattice along its base vectors $\mathbf{a_1}$, $\mathbf{a_2}$ and $\mathbf{a_3}$ at $1/h*\mathbf{a_1}$, $1/k*\mathbf{a_2}$ and $1/l*\mathbf{a_3}$. A Miller index of zero means that the referring axis will be cut in infinity. Thus, the lattice plane is parallel to this axis.
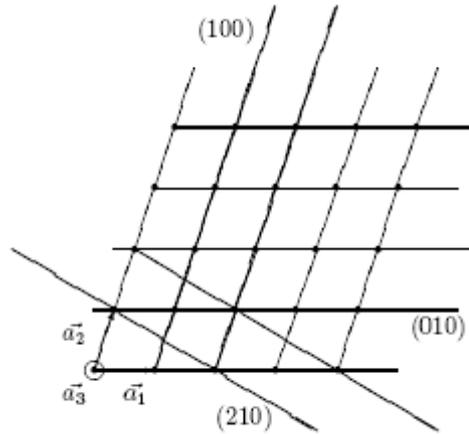
Fig. 2: Different lattice planes in a crystal lattice, $\mathbf{a_3}$ = viewing direction

The atoms in a unit cell are not rigidly fixed at their positions. They oscillate around their positions (e.g. thermal excitation). A simple description for this is the model of coupled springs. In this model atoms are connected via springs whose forces describe the binding forces between the atoms (e.g. van der Waals, Coulomb, valence). The back driving forces of the springs are proportional to the deviation x_i of the atoms from their mean positions and to the force constant D, thus. $F = -D*\Delta x$ (harmonic approximation).

Therefore, the atoms oscillate with $x_i = A_i*\sin(v*t)$ around their mean positions with the frequency v and the amplitude A_i. Both, v and A_i are influenced by the force constant D_j of the springs and the atomic masses m_i of the neighbouring atoms. The resulting lattice oscillations are called phonons in reference to the photons (light particles) in optics, which as well transport energy in dependence of their frequency. A more complex and detailed description of phonons in dependence on the lattice structure and the atomic reciprocal effects is given in lattice dynamics. In the harmonic approximation the displacements of an atom can be described with an oscillation ellipsoid. This ellipsoid describes the preferred spatial volume in which the atom is placed. Its so called mean square displacements (MSD) U^i_{jk} represent the different sizes of the ellipsoid along the different main directions j, k in the crystal. The simplest case is a sphere with the isotrope MSD B_i. In the next paragraph MSD are discussed from the point of view of diffraction analysis.

A full description of a single crystal contains information about lattice class, lattice constants and unit cell, space group and all atomic positions and their MSD. If the occupancy of one or more positions is not exactly 100%, e.g. for a mixed crystal or a crystal with deficiencies there has to be used also an occupancy factor.

3 Structure Determination with Diffraction

3.1 Introduction

Diffraction means coherent elastic scattering of a wave on a crystal. Because of the quantum mechanical wave/particle dualism x-rays as well as neutron beams offer the requested wave properties:

Electrons: $E = h\nu$; $\lambda = c/\nu$
Neutrons: $E_{kin} = 1/2 * m_n * v^2 = h\nu = p^2/2m_n$; $\lambda = h/p$; $p \sim \sqrt{(m_n\, k_B\, T)}$

h: Planck's constant; ν: oscillation frequency; λ: wavelength; c: light speed; p: impact; m_n: neutron mass; k_B: Boltzmann constant; T: temperature

Only the cross section partners are different (x-rays: scattering on the electron shell of the atoms, neutrons: core (and magnetic) scattering) as explained in detail below. In scattering experiments information about structural properties are hidden in the scattering intensities I.
In the following pages we will discuss only elastic scattering ($\lambda_{in} = \lambda_{out}$). The cross section of the radiation with the crystal lattice can be described as following:
Parallel waves of the incoming radiation with constant λ are diffracted by lattice planes which are ordered parallel with a constant distance of d. This is very similar to a light beam reflected by a mirror. The angle of the diffracted beam is equal to the angle of the incoming beam, thus the total angle between incoming and outgoing beam is 2Θ (see fig. 3).
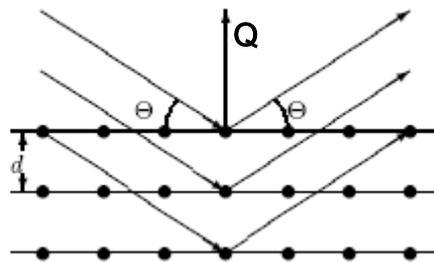
Fig. 3: Scattering on lattice planes

The overlap of all beams diffracted by a single lattice plane results in constructive interference only if the combination of the angle Θ, lattice plane distance d and wavelength λ meet*s* Bragg's law:

$$2d \sin\Theta = \lambda$$

The largest distance $d_{hkl} = |\mathbf{Q}|$ of neighboured parallel lattice planes in a crystal is never larger than the largest lattice constant $d_{hkl} \leq \max(a;\, b;\, c)$. Therefore, it can only be a few Å or less. For a cubic unit cell ($a = b = c$; $\alpha = \beta = \gamma = 90°$) this means:
$d_{hkl} = a/\sqrt{(h^2 + k^2 + l^2)}$

With increasing scattering angle also the indices (hkl) increase while the lattice plane distances shrink with a lower limit of $d_{min} = \lambda/2$. Therefore, scattering experiments need

wavelengths λ in the same order of magnitude of the lattice constants or below. This is equal to x-ray energies of about 10 keV or neutron energies about 25 meV (thermal neutrons).

Ewald Construction: In reciprocal space each Bragg reflex is represented by a point $\mathbf{Q} = h*\mathbf{a*_1} + k*\mathbf{a*_2} + l*\mathbf{a*_3}$. A scattered beam with the wave vector $\mathbf{k}$ fulfils Bragg's law if the relationship $\mathbf{k} = \mathbf{k_0} + \mathbf{Q}$, $|\mathbf{k}|=|\mathbf{k_0}|=1/\lambda$ is true, as shown in fig. 4. During an experiment the available reciprocal space can be described by an Ewald sphere with a diameter of $2/\lambda$ and the (000)-point as cross point of $\mathbf{k_0}$ direction and the centre of the diameter of the sphere. The rotation of the crystal lattice during the diffraction experiment is equal to a synchronous movement of the reciprocal lattice around the (000)-point. If Bragg's law is fulfilled, one point ($h\ k\ l$) of the reciprocal lattices lies exactly on the Ewald sphere. The angle between the $\mathbf{k}$-vector and the $\mathbf{k_0}$-vektor is 2Θ. The limited radius of $1/\lambda$ of the Ewald sphere limits also the visibility of ($h\ k\ l$) reflections to $|\mathbf{Q}| < 2/\lambda$.
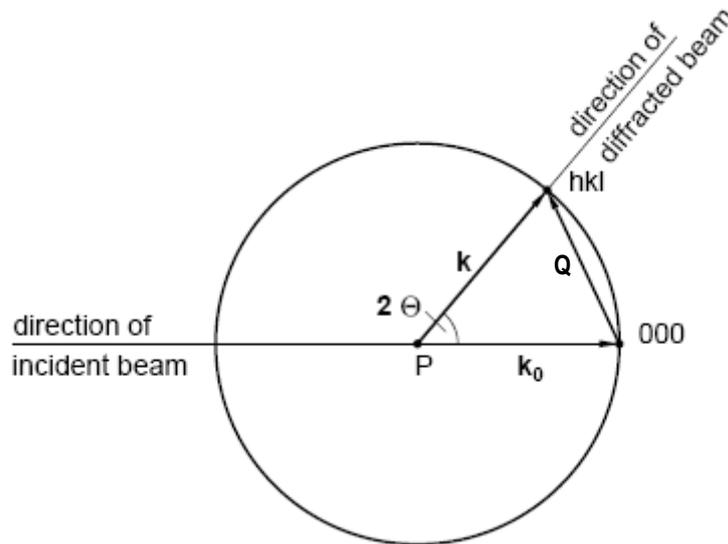
Fig. 4: Ewald construction

Determination of the Unit Cell: Following Braggs law the scattering angle 2Θ varies (for λ=const.) according to the lattice distance d_{hkl}. Thus for a given λ and known scattering angles 2Θ one can calculate the different d values of the different layers in the lattice of a crystal. With this knowledge is possible to determine the lattice system and the lattice constants of the unit cell (although not always unambiguously!).

Atomic Positions in the Unit Cell: The outer shape of a unit cell does not tell anything about the atomic positions $\mathbf{x_i}=(x_i\ y_i\ z_i)$ of each atom in this cell. To determine the atomic positions one has to measure also the quantities of the different reflection intensities of a crystal. This works because of the relationship between the intensities of Bragg reflections and the specific cross section of the selected radiation with each element in a unit cell. Generally one can use the following formula for the intensity of a Bragg reflection ($h\ k\ l$) with $\mathbf{Q}$ (kinetic scattering theory):

$I_{hkl} \sim |F_{hkl}|^2$ with $F_{hkl} = \sum_{i=1}^{n} s_i(\mathbf{Q}) \exp(2\pi\iota(hx_i+ky_i+lz_i))$

The scattering factor F is a complex function describing the overlap of the scattering waves of each atom i (n per unit cell). $s_i(\mathbf{Q})$ describes the scattering strength of the i-th atom on its position $\mathbf{x}_i$ in dependence of the scattering vector $\mathbf{Q}$, which depends on the character of cross section as described below.

In this context one remark concerning statistics: For measurements of radiation the statistical error σ is the square root of the number of measured events, e.g. x-ray or neutron particles. Thus, 100 events yield an error of 10% while 10,000 events yield an error of only 1%!

Mean Square Displacements (MSD): Thermal movement of atoms around their average positions reduce the Bragg intensities during a diffraction experiment. The cause for this effect is the reduced probability density and therefore reduced cross section probability at the average positions. For higher temperatures (above a few Kelvin) the MSD B_i of the atoms increase linearly to the temperature T, this means $B \sim T$. Near a temperature of 0 K the MSD become constant with values larger than zero (zero point oscillation of the quantum mechanical harmonic oscillator).

Thus, the true scattering capability s_i of the i-th atom in a structure has to be corrected by an angle-dependent factor (the so called Debye-Waller factor):

$$s_i(\mathbf{Q}) \rightarrow s_i(\mathbf{Q}) * \exp(-B_i(\sin \Theta_\mathbf{Q}/\lambda)^2)$$

This Debye-Waller factor decreases with increasing temperatures and yields an attenuation of the Bragg reflection intensities. At the same time this factor becomes significantly smaller with larger $\sin\Theta/\lambda \sim |\mathbf{Q}|$. Therefore, especially reflections with large indices lose a lot of intensity. The formula for anisotropic oscillations around their average positions looks like this:

$$s_i(\mathbf{Q}) \rightarrow s_i(\mathbf{Q}) * \exp(-2\pi^2(U^i_{11} h^2 a^{*2} + U^i_{22} k^2 b^{*2} + U^i_{33} l^2 c^{*2} +$$
$$+ 2U^i_{13} hl\, a^*c^* + 2U^i_{12} hk\, a^*b^* + 2U^i_{23} kl\, b^*c^*))$$

The transformation between B and U_{eq} (from the U_{ij} calculated isotropic MSD for a sphere with identical volume) yields $B = 8\pi^2 U_{\mathrm{eq}}$.

For some structures the experimentally determined MSD are significantly larger than from the harmonic calculations of the thermal movement of the atoms expected. Such deviations can have different reasons: Static local deformations like point defects, mixed compounds, anharmonic oscillations or double well potentials where two energetically equal atomic positions are very near to each other and therefore distribute the same atom over the crystal with a 50%/50% chance to one or the other position. In all those cases an additional contribution to the pure Debye-Waller factor can be found which yields an increased MSD. Therefore in the following text only the term MSD will be used to avoid misunderstandings.

3.2 Comparison of X-ray and Neutron Radiation

X-Ray Radiation interacts as electromagnetic radiation only with the electron density in a crystal. This means the shell electrons of the atoms as well as the chemical binding. The scattering capability s (atomic form factor $f(\sin\Theta/\lambda)$) of an atom depends on the number Z of its shell electrons ($f(\sin(\Theta=0)/\lambda) = Z$). To be exact, $f(\sin(\Theta)/\lambda)$ is the Fourier transform of the radial electron density distribution $n_e(r)$: $f(\sin(\Theta)/\lambda) = s \int_0^\infty 4\pi^2 n_e(r) \sin(\mu r)/\mu r\, dr$ with $\mu = 4\pi\sin(\Theta)/\lambda$. Heavy atoms with many electrons contribute much stronger to reflection

intensities ($I \sim Z^2$) than light atoms with less electrons. The reason for the $\sin\Theta/\lambda$-dependence of f is the diameter of the electron shell, which has the same order of magnitude as the wavelength λ. Because of this there is no point-like scattering centre. Thus, for large scattering angles the atomic form factors vanish and also the reflection intensities relying on them. The atomic form factors are derived from theoretical spherical electron density functions (e. g. Hartree-Fock). The resulting $f(\sin\Theta/\lambda)$-curves of all elements (separated for free atoms and ions) are listed in the international tables. Their analytical approximation can be described by seven coefficients (c; a_i; b_i; $1 \leq i \leq 3$) , see [1].

Neutron Radiation interacts with the cores and the magnetic moments of atoms. The analogue to the x-ray form factor (the scattering length b) is therefore not only dependent on the element but the isotope. At the same time b-values of elements neighboured in the periodic table can differ significantly. Nevertheless, the scattering lengths do not differ around several orders of magnitude like in the case of the atomic form factors f. Therefore, in a compound with light and heavy atoms the heavy atoms do not dominate necessarily the Bragg intensities. Furthermore the core potential with a diameter about 10^{-15}Å is a point like scattering centre and thus the scattering lengths b_n become independent of the Bragg angle and $\sin\Theta/\lambda$ respectively. This results in large intensities even at large scattering angles. The magnetic scattering lengths b_m can generate magnetic Bragg intensities comparable in their order of magnitude to the intensities of core scattering. On the other hand side the magnetic scattering lengths are strongly dependent on the $\sin\Theta/\lambda$ value due to the large spatial distribution of magnetic fields in a crystal. Therefore, it is easy to measure magnetic structures with neutrons and to separate them from the atomic structure.

Comparison: In summary in the same diffraction experiment the different characters of x-ray and neutron radiation yield different pieces of information that can be combined. X-ray scattering yield electron densities while neutron scattering reveals the exact nuclear positions. This fact is important because for polarised atoms the core position and the centre of gravity of electron densities are not identical any more. In compounds with light and heavy atoms structural changes driven by light elements need additional diffraction experiments with neutrons to reveal their influence and accurate atomic positions respectively. One has to take into account also that for x-rays intensities depend twice on $\sin\Theta/\lambda$. Once bye the atomic form factor f, and twice by the temperature dependent Debye-Waller factor (see above). The first dependence vanishes if using neutron diffraction with b=const. and decouples the structure factors from the influence of the MSD. In general this yields much more accurate MSD U_{ij} especially for the light atoms and might be helpful to reveal double well potentials.

3.3 Special Effects

From the relation $I \sim |F|^2$ one can derive that the scattering intensities of a homogenous illuminated sample increases with its volume. But there are other effects than MSD that can attenuate intensities. These effects can be absorption, extinction, polarization and the Lorentz factor:

Absorption can be described by the Lambert-Beer law:

$I = I_0 \exp(-\mu x)$, μ/cm^{-1} = linear absorption coefficient, x/cm = mean path through sample

The linear absorption coefficient is an isotropic property of matter and depends on the wavelength and kind of radiation. For x-rays penetration depths are only a few millimetre or below (e.g. for silicon with $\mu_{MoK\alpha}$=1.546 mm^{-1}, $\mu_{CuK\alpha}$=14.84 mm^{-1} with penetration depths of 3 mm and 0.3 mm respectively). This limits transmission experiments to sample diameter of typically below 0.3 mm. To correct bias of intensities due to different scattering paths through the sample one has to measure accurately the sample size in all directions. Even for sphere like samples the mean path lengths depend on 2Θ! In addition the sample environment must have an extraordinary small absorption

Thermal neutrons have for most elements a penetration depth of several centimeters. Thus, sample diameters of several millimeters and large and complex sample environments (furnaces, magnets, etc.) can be used. On the other hand side one needs sufficiently large samples for neutron diffraction which is often a delicate problem.

Extinction reduces also radiation intensities. But the character is completely different form that of absorption. In principle extinction can be explained quite easily by taking into account that each diffracted beam can be seen as a new primary beam for the neighbouring lattice planes. Therefore, the diffracted beam becomes partially backscattered towards the direction of the very first primary beam (Switch from kinetic to dynamic scattering theory!). Especially for very strong reflections this effect can reduce intensities dramatically (up to 50% and more). Condition for this effect is a merely perfect crystal.

Theoretical models which include a quantitative description of the extinction effect were developed from Zachariasen (1962) and Becker and Coppens [2, 3, 4, 5, 6]. These models base on an ideal spherical mosaic crystal with a very perfect single crystal (primary Extinction) or different mosaic blocks with almost perfect alignment (secondary Extinction) to describe the strength of the extinction effect. In addition, it is possible to take into account anisotropic extinction effect if the crystal quality is also anisotropic. Nowadays extinction correction is included in most refinement programs [7]. In general extinction is a problem of sample quality and size and therefore more commonly a problem for neutron diffraction and not so often for x-ray diffraction with much smaller samples and larger absorption.

Polarisation: X-ray radiation is electromagnetic radiation. Therefore, the primary beam of an x-ray tube is not polarized. The radiation hits the sample under an diffraction angle of Θ where it can be separated into two waves of same intensity, firstly with an electrical field vector parallel $E_{//}$ and secondly perpendicular $E_{\perp}$ towards the Θ-axis. Whilst the radiation with $E_{//}$ will not be attenuated the radiation with $E_{\perp}$ will be attenuated with $E_{\perp} \rightarrow \cos(2\Theta)\, E_{\perp}$. The polarization factor P for the attenuation has then the following formula ($I \sim E^2$):

$$P = (1+\cos(2\Theta)^2)/2$$

Additional optical components like monochromator crystals also have an impact on the polarization and have to be taken into account accordingly.

Lorentz factor: The Lorentz factor L is a purely geometrical factor describing that the movement during an ω- and Θ-scan respectively for identical angular speeds $\Delta\omega/\Delta t$ results in an effectively elongated stay of the sample in the reflection position towards higher 2Θ with:

$$L = 1/\sin(2\Theta)$$

This has to be taken into account for any kind of radiation in a diffraction experiment.

3.4 Summary of Theory of Method

The different interactions of x-ray and neutron radiation with the atoms in a crystal make neutrons in general the better choice for a diffraction experiment. But on the other hand one has to take into account the available flux of x-rays and neutrons respectively. The flux of modern neutron sources like the Heinz Maier-Leibnitz neutron source (FRM II) is spread around a broad spectrum of neutron energies. In a sharp band of energies/wavelengths, e.g. $\Delta\lambda/\lambda < 10^{-3}$, the flux of neutrons is several order of magnitude smaller than the flux of x-rays of a corresponding synchrotron source or x-ray tube in the laboratory. The reason for this is that in an x-ray tube most x-rays are generated in a small energy band, the characteristic lines of the tube target (K_α, K_β, etc.). Additional metal foils used as filters cut off unwanted characteristic lines yielding quasi monochromatic radiation of a single wavelength.

To use neutrons around a small energy band one has to use monochromator crystals. This reduces significantly the number of available neutrons for the diffraction experiment. Thus, the weak flux of neutrons and the weak cross sections of neutrons with matter have to be compensated by large sample sizes of several millimeters. For the same reason the monochromatisation of the neutrons is normally chosen to be not too sharp (resolution about $\Delta\lambda/\lambda \approx 10^{-2} - 10^{-3}$ for neutrons, $\Delta\lambda/\lambda \approx 10^{-5} - 10^{-6}$ for synchrotron).

3.5 From Measurement to Model

To get a structural model from the experimentally collected integral Bragg intensities one needs several steps in advance. Firstly on has to make sure that all reflections are measured properly (no shading, no $\lambda/2$-contamination, no Umweganregung (Renninger effect)). Damaged reflections have to be excluded from further treatment.

During data refinement not only the quantities of the relative intensities but also their errors are taken into account. The total statistical error σ of an integral intensity I_{obs} of a reflection with n_{total} data points I_j is calculated as following (assuming each $I_j=P_j+B_j$ consists of two components for profile P_j and background B_j with $I_{obs}=\sum^{n\_total}_{j=1} P_j$, $I_{background}=\sum^{n\_total}_{j=1} B_j$) [9]:

$$\sigma^2 = I_{obs} + (n_{total}-n_{background})/n_{background}*I_{background} + (k\,I_{total})^2$$

The first two components refer to the error caused by counting statistics only. It contains the effective intensity I_{obs} and the contribution of the background with a statistical correction factor. Other effects that influence the reproducibility of a measurement (and thus the total error), e. g. specific errors of the instrumental adjustment, are collected in the so called *McCandlish factor k* and contribute also to the total error. Therefore, the total error cannot drop below the physically correct limit of the experiment and thus the impact of strong reflections does not become exaggerated in the refinement. The determination of *k* is done by measuring the same set of reflections several times during an experiment (the so called standard reflections). The mean variation of the averaged value represents *k*. In addition, repeated measurements of standard reflections allow the detection of unwanted changes during experiment like structural changes or an unintended change of the sample orientation.

To make sure the comparability of all reflections with each other, all intensities and errors are normalized to the same time of measurement (or monitor count rate) and undergo the Lorentz and (in the x-ray case) polarization correction.

Finally in advance of the data refinement there can be done by a numerical (e.g. with Tbar/DataP, [8]) or an empirical absorption if necessary. The quality of a measurement is checked in advance of the data refinement by comparing symmetry equivalent reflections and systematic extinctions to confirm the Laue group and space group symmetry. The result is written as internal *R*-value:

$$R_{\text{int}} = (\textstyle\sum_{k=1}^{m}(\sum_{j=1}^{n}{}_k\,(<I_k>-I_j)^2))/\,(\sum_{k=1}\sum_{j=1}^{n}{}_k(I_j^2)_k)$$

R_{int} represents the mean error of a single reflection *j* of a group *k* of n_k symmetry equivalent reflections, corresponding to its group and the total number m of all symmetrically independent groups. Therefore R_{int} is also a good mark to check the absorption correction. After these preliminary steps one can start the final data refinement.

At the beginning one has to develop a structural model. The problem with that is that we measure only the absolute values $|F_{\text{hkl}}|$ and not the complete structure factor $F_{\text{hkl}} = |F_{hkl}|\exp(\iota\phi)$ including its phase ϕ. Therefore, generally the direct Fourier-transformation of the reflection information F_{hkl} from reciprocal space into the density information ρ in the direct space (electron density for x-rays, probability density of atomic cores for neutrons) with

$$\rho(\mathbf{x}) \sim \textstyle\sum_h\sum_k\sum_l F_{hkl}\exp(-2\pi(hx+ky+lz))$$

is not possible. This can be done only by direct methods like Patterson, heavy atom method or anomalous dispersion for x-rays.

In the so called refinement program a given structural model (space group, lattice constants, atomic form factors, MSD, etc.) are compared with the experimental data and fitted. In a leas squares routine those programs try to optimize (typically over several cycles) the free parameters to reduce the difference between the calculated structure factors F_{calc} and intensities $|F_{calc}|^2$ respectively and the experimentally found F_{obs} and $|F_{\text{obs}}|^2$ respectively. To quantise the quality of measurement there are several values in use:

1. *Unweighted R*-value: $R_{\text{u}} = \sum_{hkl} |F_{\text{obs}}^2 - F_{\text{calc}}^2|/\sum_{hkl} F_{\text{obs}}^2$
This value gives the alignment of the whole number of reflections without their specific errors.

2. *Weighted R*-value: $R_{\text{w}} = (\sum_{hkl} w\,(F_{\text{obs}}^2 - F_{\text{calc}}^2)^2)/\sum_{hkl} w\,F_{\text{obs}}^4$
This value represents the alignment of the whole number of reflections including their specific errors or weights ($w\sim1/\sigma^2$). Sometimes weights are adopted in a way to suppress unwanted influence of the refinement algorithm by weak or badly defined reflections. Be aware that such corrections have to be done extremely carefully because otherwise the refinement adopts the data to the selected structural model and not the model to the experimental data!

3. *Goodness of Fit S*: $S^2 = (\sum_{hkl} w\,(F_{\text{obs}}^2 - F_{\text{calc}}^2)/(n_{\text{hkl-reflections}} - n_{\text{free parameter}})$

S should have a value near one if the weighting scheme and the structure model fit to the experimental data set.

4 Sample Section

4.1 Introduction

$La_{2-x}Sr_xCuO_4$ is one of the cuprate superconductors with K_2NiF_4- structure for whose discovery the noble prize was granted in 1988 (Bednorz and Müller [10]). Pure La_2CuO_4 is an isolator. Doping with earth alkali metals (Ca^{2+}, Sr^{2+}, Ba^{2+}) on the La^{3+} lattice positions generates in dependence of the degree of doping superconductivity. Sr doping of $x=0.15$ yields a maximum T_c of 38 K.

Pure La_2CuO_4 undergoes at $T_{t-o}=530$ K a structural phase transition from the tetragonal high temperature phase (HTT)

$F4/mmm$: $a=b=5.384$ Å, $c=13.204$ Å, $\alpha=\beta=\gamma=90°$ at $T=540$ K

to the orthorhombic low temperature phase (LTO)

$Abma$: $a=5.409$ Å, $b=5.357$ Å, $c=13.144$ Å, $\alpha=\beta=\gamma=90°$ at room temperature.

The phase transition temperature T_{t-o} drops for $La_{2-x}Sr_xCuO_4$ with increased doping and disappears above $x=0.2$.
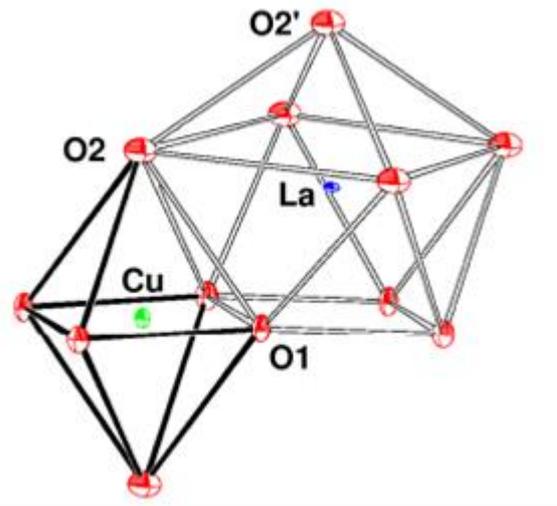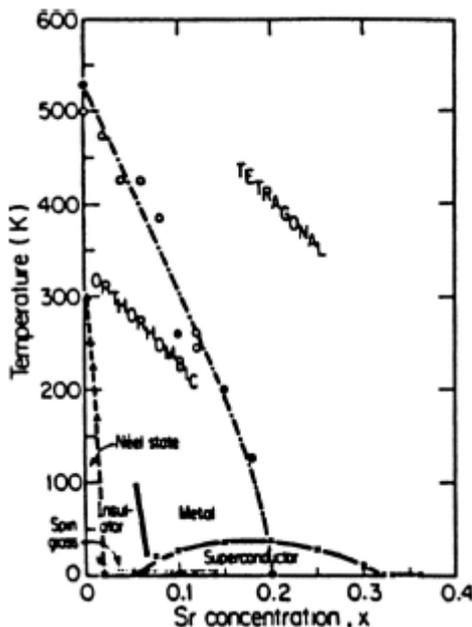
Fig.. 6 left: J. Birgenau, G. Shirane, HTC Superconductors I, World Scientific (1989)
Fig.. 6 right: Structural parts of La_2CuO_4 in the LTO phase
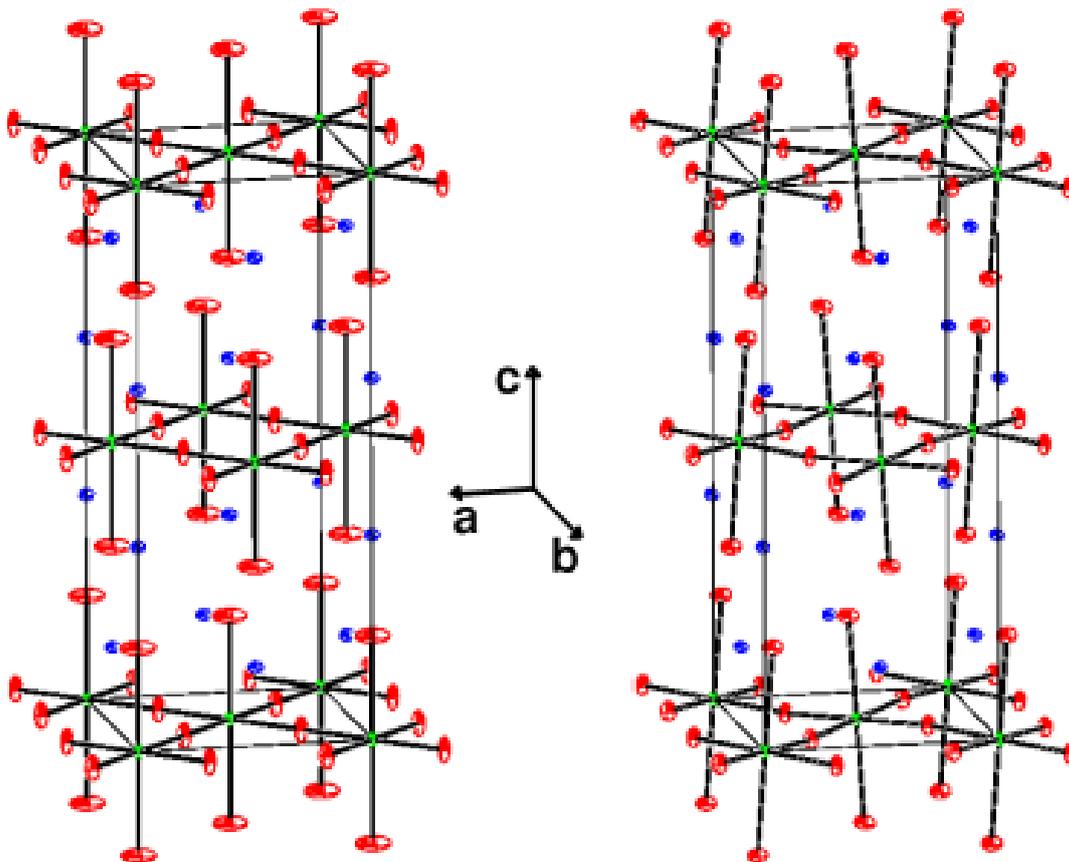
Fig. 7 left: tetragonal HTT phase   Fig. 7 right: orthorhombic LTO phase

4.2 Twinning

During the transition into the low temperature phase the CuO_6 octahedrons are tilted around their [010] axis. Thus, the two axes of identical length in the HTT phase, a_1 and a_2, are not equal in the LTO phase anymore. Instead, the longer one becomes the new a axis, the shorter one becomes the b axis. Whether a_1 or a_2 becomes the new a axis depends only on the real structure of the crystal, for instance grain boundaries or point defects. Therefore, one can find two equivalent crystallographic space groups in the LTO phase:

Abma $(a_1 \rightarrow a, a_2 \rightarrow b)$ and B*mab* $(a_1 \rightarrow b, a_2 \rightarrow a)$

For the structure factors in the LTO is valid:

$F_{Abma}(hkl) = F_{Bmab}(khl)$
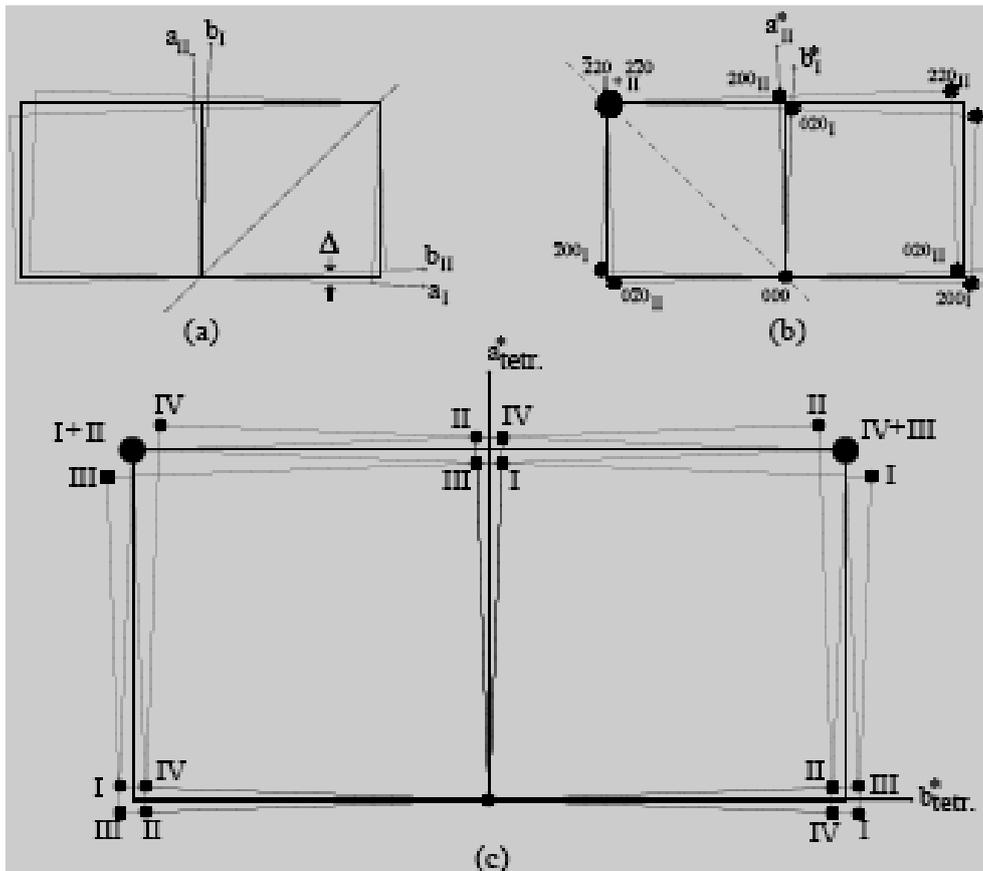
Fig. 8
- (a) orthorhombic distortion with twinning corresponding to a (1-10) mirroring
- (b) corresponding reciprocal lattice
- (c) Overlay of (110)- and (1-10)-mirroring in reciprocal space

In the HTT phase only reflections with *h, k, l* of equal parity (*g* for even, *u* for uneven) are allowed - (*uuu*) and (*ggg*). They are called in the following main structure reflections.

In the LTO phase additional reflections occur, called super structure reflections: In the *Abma*-Structure (*ugg*), l≠0 and (*guu*), in the *Bmab* structure (*gug*), l≠0 and (*ugu*).

Forbidden in both the HTT and the LTO phase are (*uug*), (*ggu*), (*ug*0) and (*gu*0).

These extinction rules will become important later.

In the real structure of the crystal there exist four domain types in total. They are separated into two pairs with the couple *Abma₁/Bmab₁* (I/II) with the (1-10) mirror plane as grain boundary and the couple *Abma₂/Bmab₂* (III/IV) with the (110) mirror plane as grain boundary (fig. 8).

The following overlaps of reflections result from this twinning:

- No splitting of the (00l) reflections,
- triple splitting of the (hh0) reflections
- fourfold splitting of the (h00) reflections.

An equal distribution of the volumetric portion of each single domain yields a ratio of intensities of 1:2:1 for the triple splitting. The distance $\Delta\omega$ between the centre and the side

peaks of a (*hkl*) reflex gives because of $(a+b)/2 = a_{1/2}$ an information about the orthorhombic *a/b* splitting. For the triple splitting of a (*hh*0) reflex is valid:

$$\Delta\omega = 90° \text{-} 2\arctan(b/a)$$

Thus, although the real crystal is twinned, one can quantify the orthorhombic distortion.

The intensity contribution of the single domains corresponding to the whole intensity of a reflection can be described (taking into account the incoherent overlap of single intensities and the volumetric portions V_{A1} to V_{B2} of the domains) as follows:

$$I_{\text{obs}}(hkl) = I_{Abma1}(hkl) + I_{Bmab1}(hkl) + I_{Abma2}(hkl) + I_{Bmab2}(khl) \text{ or}$$

$$V_{\text{total}}|F_{\text{obs}}(hkl)|^2 = V_{A1}|F_{Abma1}(hkl)|^2 + V_{B1}|F_{Bmab1}(hkl)|^2 + V_{A2}|F_{Abma2}(hkl)|^2 + V_{B2}|F_{Bmab2}(hkl)|^2$$

$$= (V_{A1} + V_{A2})|F_{Abma1}(hkl)|^2 + (V_{B1} + V_{B2})|F_{Bmab1}(hkl)|^2$$

$$= V_{\text{total}} \{ \alpha|F_{Abma}(hkl)|^2 + (1\text{-}\alpha) |F_{Abma}(khl)|^2 \}$$

with α being the relative portion of the volume of *Abma* domains to the crystal..

Because of the extinction rules in the LTO phase for the super structure reflections is valid: $I_{\text{obs}}(hkl) \sim \alpha|F_{Abma}(hkl)|^2$ for *Abma* and $I_{\text{obs}}(hkl) \sim (1\text{-}\alpha)|F_{Abma}(khl)|^2$ for *Bmab*. Thus, one can classify directly intensities to the volumetric portions of the domain types *Abma* and *Bmab* respectively. Therefore, by using one single additional parameter α to describe the relation between the twins in the structure one can determine the orthorhombic single crystal structure! This holds true although the Bragg reflections contain contributions of up to four different domains.

4.3 Oxygen Position

The oxygen atoms undergo the largest shift of their positions during the transition to the LTO phase. For the structure factor of any Bragg reflection forbidden in *F4/mmm* is valid:

$$F(hkl) \sim \sum_i s_i \exp(-2\pi\iota(hx_i+ky_i+lz_i)) = F(hkl)_{\text{apex oxygen}}+F(hkl)_{\text{in plane oxygen}}+F(hkl)_{\text{structure w/o O}}$$
$$\rightarrow F(hkl)_{\text{apex oxygen}}+F(hkl)_{\text{in plane oxygen}}$$

In the LTO phase the atomic position of the apex oxygen is (x 0 z), the atomic position for the in-plane oxygen is (1/4 1/4 -z). This yields the following intensities for the superstructure reflections:

$F(hkl)_{\text{apex oxygen}} = \cos(2\pi hx)\cos(2\pi lz)$ for *h* even or
$F(hkl)_{\text{apex oxygen}} = \sin(2\pi hx)\cos(2\pi lz)$ for *h* uneven

In the case of x-rays the form factor $f_i \sim Z_i$, Z_i=order number is much smaller for oxygen (Z=16) than for Cu (Z=29) and La (Z=57). Because of $I_{\text{obs}}(hkl) \sim |F(hkl)|^2$ the oxygen shift is hardly measurable. In the case of neutrons the scattering lengths b_i of all atoms are in the same order of magnitude (b_O=5.803 barn, b_{Cu}= barn, b_{La}= barn, 1 barn = 10^{-24} cm^{-2}). Therefore, the intensity contribution of the oxygen atoms increases in relation to the other elements in the structure and allows a much more precise determination of the structural change of the oxygen positions

5   Preparatory Exercises

1. What is the fundamental difference between powder/single crystal diffraction and what are the advantages and disadvantages of both techniques (Compare d-values and orientations of different reflections in a cubic structure)?

2. What is wrong with fig. 2?

3. Which reflections are not allowed in a face centered structure (structure factor)?

4. There is no space group F4/mmm in the international tables. Why (Which other space group in the international tables yields the same pattern in direct space)?

6   Experiment Procedure

During this practical course not all physical and technical aspects of structure analysis with neutrons can be discussed in detail. Nevertheless this course is supposed point out the basic similarities and dissimilarities of x-rays and neutron radiation as well as their specific advantages and disadvantages in general and referring to single crystal diffraction. The sample selected for this practical course is most suitable for this purpose because of its special crystallographic peculiarities.

6.1   The Instrument

Fig. 5 shows the typical setup of a single crystal diffractometer with a single detector. Outgoing from the radiation source a primary beam defined by primary optics (in our case the beam tube) reaches the single crystal sample. If one lattice plane (*hkl*) fulfils Braggs laws, the scattered beam, called secondary beam, leaves the sample under an angle 2Θ to the primary beam. The exact direction of this beam depends only on the relative orientation of the sample to the primary beam.

For the diffractometer shown in fig. 5 the movement of the neutron detector is limited to a horizontal rotation around the 2Θ axis. Thus, only those reflections can be measured, whose scattering vector **Q** lies exactly in the plane defined by the source, the sample and detector circle. This plane is also called scattering plane.
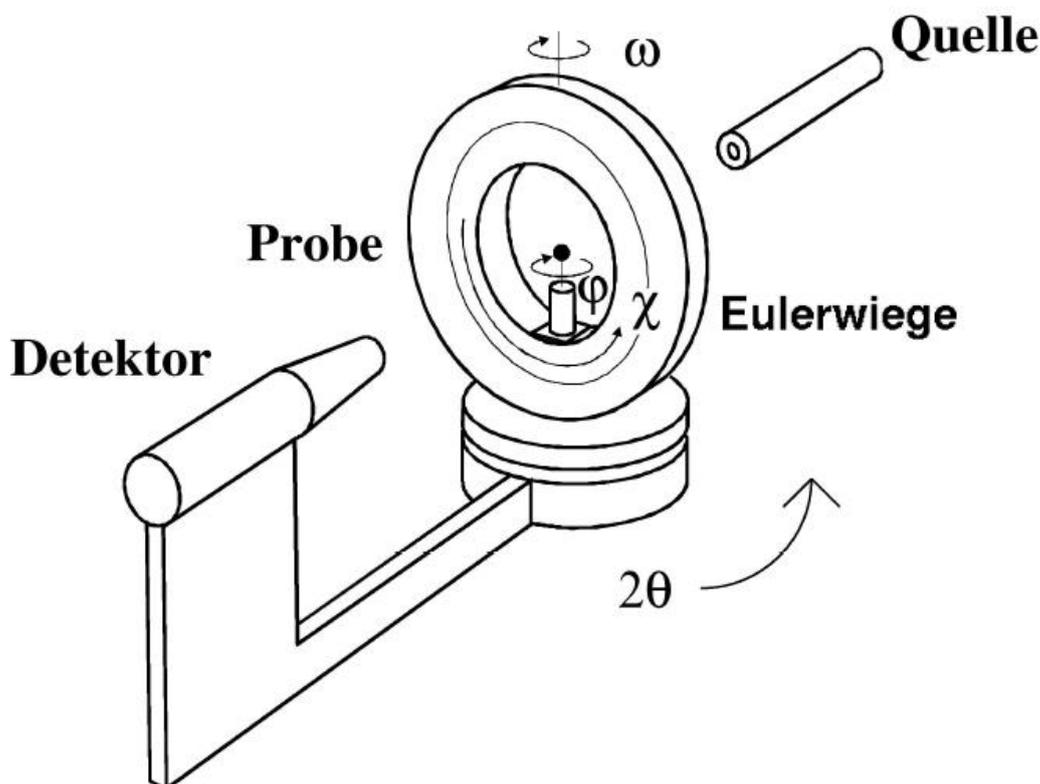
Fig. 5: Scheme of a single crystal diffractometer

To direct the secondary beam towards the detector position one has to orient the sample around the three axes ω, χ and ϕ. These three axes allow a virtually random orientation of the crystal in the primary beam. During the experiment the sample has to stay exactly in the cross point of all four axes (2Θ, ω, χ and ϕ) and the primary beam. Additionally, for 2Θ = ω = χ = ϕ = 0° the primary beam direction and the χ axis on one hand side and the 2Θ-, ω- and ϕ-axes on the other hand side are identical while the angle between the primary beam and the 2Θ-is exactly 90°. Because of the four rotational axes (2Θ, ω, χ, ϕ) this kind of single crystal diffractometer is often called four circle diffractometer. Another often used geometry - the so called κ geometry - will not be discussed in detail here.

Further details of the experimental setup:

1. Beam source and primary optics: The primary beam is generated by a suitable source (x-rays: x-ray tube, synchrotron; neutrons: nuclear fission, spallation source). The primary optics defines the path of the beam to the sample in the Eulerian cradle. Furthermore, the primary optics defines the beam diameter using slits to make it fit to the sample size for homogeneous illumination. This homogeneity is very important because the quality of the data refinement relies on the comparison of the intensity ratios between the different reflections measured during an experiment. Wrong ratios caused by inhomogeneous illumination can yield wrong structural details! Other components of the primary optics are collimators defining beam divergence and filters or monochromators which define the wavelength λ of the radiation.

2. Sample and sample environment: The sample position is fixed by the centre of the Eulerian cradle which is defined by the cross point of the axes ω, χ and ϕ. As described above, the cradle itself has in combination with the ω-circle the task to orient the sample according to the observed reflection in a way that it hits the detector. The sample itself is mounted on a goniometer head. This head allows the adjustment of the sample in all three directions **x**; **y**; **z**, via microscope or camera. To avoid scattering from the sample environment and goniometer head the sample is usually connected to the head via a thin glass fibre (x-rays) or aluminium pin (neutrons). This reduces significantly background scattering. For experiments at high or low temperatures adjustable cooling or heating devices can be mounted into the Eulerian cradle.

3. Secondary optics and detector: The 2Θ arm of the instrument hold the detector which – in the ideal case – catches only radiation scattered from the sample and transforms it to an electrical signal. There exists a variety of detectors, single detectors and position sensitive 1D and 2D detectors. Area detectors have a large sensitive area that allows the accurate observation of spatial distribution of radiation. Other components of the secondary optics are slits and collimators or analyser (as optional units). They fulfil the task to shield the detector from unwanted radiation like scattering from sample environment, scattering in air, wrong wavelengths or fluorescence

6.2   Sequence of measurement in Theory

1. Centering: In advance of the planned scientific program (profile analysis, Bragg data collection) the orientation of the sample in relation to the coordinate system of the diffractometer has to be determined. First of all the sample has to be centered optically to assure a homogeneous illumination of the sample. Afterwards, a reflection search routine has to be started to optimize the intensity of a found reflection by moving several angles after each other.

In many cases there are some structural information like the unit cell and hkl values of strong reflections available from previous studies, e.g. from powder diffraction, thus, one can limit the reflection search to 2Θ values around these strong reflections to spare some time and to classify manually the found reflections with the correct indices.

2. Determination of orienting matrix and lattice constants: The comparison of the $\mathbf{Q}$ vectors of the found and centered reflections yields generally one or more suggestions for a suitable unit cell. This is done by a least squares routine minimizing the error bars between the calculated and measured $\mathbf{Q}$ vectors. This method allows to determine accurately the orientation matrix $\mathbf{M_o} = (\mathbf{a^*}\ \mathbf{b^*}\ \mathbf{c^*})^T$ of the sample relative to the coordinate system of the diffractometer and the lattice constants of the unit cell.

On HEiDi the axes are defined as following: $\mathbf{x}$=primary beam, $\mathbf{z} \parallel 2\Theta$ axis, $\mathbf{y}=\mathbf{z} \times \mathbf{x}$.
A proposed unit cell is only acceptable if all experimentally found reflections can be indexed with integer *hkl* , this means $\mathbf{Q} = (h\ k\ l)*\mathbf{M_o}$. In addition the found reflection intensities *I* offer a course check, e.g. whether extinction rules are followed or intensities of symmetrically identical reflections are identical.

3. Profile analyses and scan types: During profile analysis reflex profiles are analysed via so called ω scans. During this scan the sample is turned for *n* steps around a center position ω_0. This scan makes different crystallites in one large sample visible. In addition one has to take into account that even in perfectly grown crystals there are grain boundaries and slight mismatches of the crystallites. These mosaic blocks are perfect crystals whose orientations are misaligned only a few tenths of a degree or less. By the way, the axis position $2\Theta/2=\Theta=\omega$ is called the bisecting orientation of the Eulerian cradle.

As long as the vertical aperture is large enough, a rotation of the crystal around a ω_0, that is equivalent to the ideal Θ_0 Bragg angle of a reflex allows to catch the intensity portion of each crystallite in the sample in the neutron detector on the fixed 2Θ position, even those that can only be found for slightly differing ω. Therefore, a crystal with large mosaicity gives measurable intensities over a broader ω area than a perfect crystal. Thus it gives a broader reflex profile. Also the tearing and cracking of a crystal creates broad but irregular profiles.

Beside the crystal quality also the instrumental resolution limits the measurable profile widths in the following sense: The divergence of a primary beam in real experiment is limited, for instance to 0.2°.

If a reflection fulfils Bragg's Law at Θ, the total divergence is a convolution of the divergence of the primary beam *and* the mosaicity/divergence of the sample. Thus, the reflection profile will never be sharper than the divergence of the primary beam itself.

In addition one has to take into account that for larger diffraction angles a fixed detector window will not be sufficient to catch the whole reflection intensities during a rocking scan.

For a given spectrum $\Delta\lambda/\lambda$ of the primary beam, with increasing scattering angle Θ angular range $\Delta\Theta$ increases with $\sin(\Delta\Theta/2)=\tan(\Theta)*\Delta\lambda/\lambda$ for which all wavelengths in the interval $\lambda\pm\Delta\lambda/2$ fulfilling Bragg's law are distributed. Because of the limited width of the detector window this yields a cut off of intensities for larger scattering angles for ω-scans.

To compensate this cut off effect it is necessary to begin at a certain 2Θ-angle to move the detector window with the ω-angle.. This can be done by so called $\omega/2\Theta$-scans. The start position of this 2Θ range depends on the primary beam divergence and sample quality and has to be checked individually for each sample.

4. Collection of Bragg reflections: If a sample was found good after the described preliminary studies one can start with the Bragg data collection. In this data collection all (or selected) reflections in a given 2Θ interval are collected automatically. The usual strategy follows the rule „Only as many as necessary". This means the following: On one hand side the quality of the measured reflections has to fulfil certain standards (like small standard deviations σ and a good shape of the profiles) to reach an acceptable accuracy. On the other side there is only a limited amount of time available for each reflection due to the huge number of them (up to several thousands). and the limited beam time. A rule of thumb is therefore to measure about 10 non symmetry equivalent reflections for each free parameter used in the data refinement to get the correct structure. To achieve this goal a typical algorithm is to do a prescan with t_{min} per point of measurement in combination with a given larger (e.g. $I/\sigma=4$ and 25%, respectively) and a smaller (e.g. $I/\sigma=20$ and 5%, respectively) relative error limit. t_{min} is chosen in a way that the statistics of strong reflections is fine already after the prescan. Weak reflections are also noticed in the prescan and stored as weak reflections without additional treatment. To improve the statistics of those reflections in between one performs a second scan with a limited amount of time up to t_{max}- t_{min}. This method avoids spending unreasonable beam time to weak reflections which will not help to improve the quality of the structure model.

6.3   and in Practice

1. **Adjust optically the sample in the neutron beam:** Alignment of the sample in the rotational centre of the instrument. This is necessary for a homogeneous illumination of the sample for all possible orientations.

2. **Search for Bragg reflections and center them, , "Reflex centering**": Sample and detector position are controlled by special diffractometer software. The main goal is to find suitable angular positions for the detector first and afterwards for the sample to get a measurable signal. Afterwards the orientation of the sample in the Eulerian cradle has to be optimized for maximum intensity.

3. **Analyse profiles of selected reflections:** Study different reflex profiles and reveal the impact of twinning

4. **Determine the orthorhombic lattice parameters a, b and c**: Estimate the misalignment between *a* and *b* in reference to $a_{1/2}$ in the real tetragonal cell.

5. **Determine the average tetragonal unit cell**: The centering of different reflections allows the calculation of all lattice constants including the averaged tetragonal parameters.

6. **Observe super structure reflections:** Measuring pairs of (*hkl*)/(*khl*) allows the estimation of the volumetric contribution of each single domain to the whole crystal.

7. **Select measurement parameters for Bragg data collection:** In order to optimize the number and statistical quality of collected Bragg reflections suitable scan parameters (time/step, no. of steps, step widths, etc.) have to be determined.

8. **Collect a Bragg data set**

6.4 Data analysis

After having measured a Bragg data set one has to do the final step, the alignment of model and measurement:

1. **Data Reduction:** In this process the measured reflection profiles are analysed and reduced to a simple list of all measured reflections and their integrated intensities including error bars and some other useful information. This so-called *hkl*-list is the base for the next step:

2. **Structure refinement:** Here the measured *hkl*-list and our structure model are combined to determine structural details like atomic positions and mean square displacements.

7   Experiment-Related Exercises

1. Why is the optical adjustment of the sample so important?
2. How large is the *a/b*-splitting at room temperature $(=|a-b|/(a+b))$?
3. What is the benefit/enhancement of studying the room temperature structure with neutrons instead of X-rays?

References

[1]　Th. Hahn (ed.), Space-group symmetry, International Tables for Crystallography Vol. A, Kluver Academic Publishers (2006).

[2]　W.H. Zachariasen, Acta Cryst. 18, 703 (1965).

[3]　W.H. Zachariasen, Acta Cryst. 18, 705 (1965).

[4]　P. Coppens and W.C. Hamilton, Acta Cryst. A 26, 71-83 (1970).

[5]　P.J. Becker and P. Coppens, Acta Cryst. A 30, 129-147 (1974).

[6]　P.J. Becker and P. Coppens, Acta Cryst. A 30, 148-153 (1974).

[7]　U.H. Zucker, E. Perrenthaler, W.F. Kuhs, R. Bachmann and H. Schulz J. of Appl. Crystallogr., 16, 358 (1983).

[8]　P. Coppens, W.C. Hamilton, S. Wilkins, M.S. Lehmann and Savariault, Datap, http://www.ill.fr/data treat/diftreat.html#single (1999).

[9]　M.S. Lehmann, F.K. Larsen, Acta Cryst. A 30, 580-584 (1974)

[10]　J. Bednorz and K. Müller, Z. Phys. B 64, 189 (1986).

Literature

N.W. Ashcroft and N.D. Mermin, Festkörperphysik, Oldenbourg 2001.

H. Ibach and H. Lüth, Festkörperphysik, Einführung in die Grundlagen, 6. Edition Springer 2002.

C. Kittel, Einführung in die Festkörperphysik, 10. Edition, Oldenbourg 1993.

W. Borchardt-Ott, Kristallographie. Eine Einführung für Naturwissenschaftler, 6. Auflage Springer 2002.

W. Kleber, Einführung in die Kristallographie, Oldenbourg 1998

H. Dachs, Neutron Diffraction, Springer (1978)

D.J. Dyson, X-Ray and Electron Diffraction Studies in Material Science, Maney Pub 2004.

C. Giacovazzo, Fundamentals of Crystallography, 2nd Ed., Oxford University Press 2002.

L.A. Aslanov, Crystallographic Instrumentation, Oxford University Press 1998.

M.T. Dove, Structure and Dynamics. An Atomic View of Materials, Oxford University Press 2003. W. Clegg, Crystal Structure Analysis. Principles and Practice, Oxford University Press 2001.

Appendix (Tables and space groups from [1])

3.1. SPACE-GROUP DETERMINATION AND DIFFRACTION SYMBOLS

Table 3.1.4.1. *Reflection conditions, diffraction symbols and possible space groups* (*cont.*)

ORTHORHOMBIC, Laue class *mmm* (2/m 2/m 2/m) (*cont.*)

Reflection conditions								Laue class *mmm* (2/m 2/m 2/m)		
								Point group		
hkl	*0kl*	*h0l*	*hk0*	*h00*	*0k0*	*00l*	Extinction symbol	222	*mm2* *m2m* *2mm*	*mmm*
	$k+l$	l	k		k	l	$Pncb$			$Pncb$ (50)
	$k+l$	l	$h+k$	h	k	l	$Pncn$			$Pncn$ (52)
	$k+l$	$h+l$		h	k	l	$Pnn-$		$\boldsymbol{Pnn2}$ (34)	$\boldsymbol{Pnnm}$ (58)
	$k+l$	$h+l$	h	h	k	l	$Pnna$			$\boldsymbol{Pnna}$ (52)
	$k+l$	$h+l$	k	h	k	l	$Pnnb$			$\boldsymbol{Pnnb}$ (52)
	$k+l$	$h+l$	$h+k$	h	k	l	$Pnnn$			$\boldsymbol{Pnnn}$ (48)
$h+k$	k	h	$h+k$	h	k		$C---$	$\boldsymbol{C222}$ (21)	$\boldsymbol{Cmm2}$ (35) $Cm2m$ (38) $C2mm$ (38)	$\boldsymbol{Cmmm}$ (65)
$h+k$	k	h	$h+k$	h	k	l	$C--2_1$	$\boldsymbol{C222_1}$ (20)		
$h+k$	k	h	h,k	h	k		$C--(ab)$		$Cm2e$ (39) $C2me$ (39)	$\boldsymbol{Cmme}$ (67)
$h+k$	k	h,l	$h+k$	h	k	l	$C-c-$		$\boldsymbol{Cmc2_1}$ (36) $C2cm$ (40)	$\boldsymbol{Cmcm}$ (63)
$h+k$	k	h,l	h,k	h	k	l	$C-c(ab)$		$C2ce$ (41)	$\boldsymbol{Cmce}$ (64)
$h+k$	k,l	h	$h+k$	h	k	l	$Cc--$		$Ccm2_1$ (36) $Cc2m$ (40)	$Ccmm$ (63)
$h+k$	k,l	h	h,k	h	k	l	$Cc-(ab)$		$Cc2e$ (41)	$Ccme$ (64)
$h+k$	k,l	h,l	$h+k$	h	k	l	$Ccc-$		$\boldsymbol{Ccc2}$ (37)	$\boldsymbol{Cccm}$ (66)
$h+k$	k,l	h,l	h,k	h	k	l	$Ccc(ab)$			$\boldsymbol{Ccce}$ (68)
$h+l$	l	$h+l$	h	h		l	$B---$	$B222$ (21)	$Bmm2$ (38) $Bm2m$ (35) $B2mm$ (38)	$Bmmm$ (65)
$h+l$	l	$h+l$	h	h	k	l	$B-2_1-$	$B22_12$ (20)		
$h+l$	l	$h+l$	h,k	h	k	l	$B--b$		$Bm2_1b$ (36) $B2mb$ (40)	$Bmmb$ (63)
$h+l$	l	h,l	h	h		l	$B-(ac)-$		$Bme2$ (39) $B2em$ (39)	$Bmem$ (67)
$h+l$	l	h,l	h,k	h	k	l	$B-(ac)b$		$B2eb$ (41)	$Bmeb$ (64)
$h+l$	k,l	$h+l$	h	h	k	l	$Bb--$		$Bbm2$ (40) $Bb2_1m$ (36)	$Bbmm$ (63)
$h+l$	k,l	$h+l$	h,k	h	k	l	$Bb-b$		$Bb2b$ (37)	$Bbmb$ (66)
$h+l$	k,l	h,l	h	h	k	l	$Bb(ac)-$		$Bbe2$ (41)	$Bbem$ (64)
$h+l$	k,l	h,l	h,k	h	k	l	$Bb(ac)b$			$Bbeb$ (68)
$k+l$	$k+l$	l	k		k	l	$A---$	$A222$ (21)	$\boldsymbol{Amm2}$ (38) $Am2m$ (38) $A2mm$ (35)	$Ammm$ (65)
$k+l$	$k+l$	l	k	h	k	l	$A2_1--$	$A2_122$ (20)		
$k+l$	$k+l$	l	h,k	h	k	l	$A--a$		$\boldsymbol{Am2a}$ (40) $A2_1ma$ (36)	$Amma$ (63)
$k+l$	$k+l$	h,l	k	h	k	l	$A-a-$		$\boldsymbol{Ama2}$ (40) $A2_1am$ (36)	$Amam$ (63)
$k+l$	$k+l$	h,l	h,k	h	k	l	$A-aa$		$A2aa$ (37)	$Amaa$ (66)
$k+l$	k,l	l	k		k	l	$A(bc)--$		$\boldsymbol{Aem2}$ (39) $Ae2m$ (39)	$Aemm$ (67)
$k+l$	k,l	l	h,k	h	k	l	$A(bc)-a$		$Ae2a$ (41)	$Aema$ (64)
$k+l$	k,l	h,l	k	h	k	l	$A(bc)a-$		$\boldsymbol{Aea2}$ (41)	$Aeam$ (64)
$k+l$	k,l	h,l	h,k	h	k	l	$A(bc)aa$			$Aeaa$ (68)
$h+k+l$	$k+l$	$h+l$	$h+k$	h	k	l	$I---$	$\begin{bmatrix}\boldsymbol{I222}\ (23) \\ \boldsymbol{I2_12_12_1}(24)\end{bmatrix}_*$	$\boldsymbol{Imm2}$ (44) $Im2m$ (44)	$\boldsymbol{Immm}$ (71)

3. DETERMINATION OF SPACE GROUPS

Table 3.1.4.1. Reflection conditions, diffraction symbols and possible space groups (cont.)

ORTHORHOMBIC, Laue class *mmm* (2/m 2/m 2/m) (*cont.*)

		Reflection conditions						Laue class *mmm* (2/m 2/m 2/m)		
									Point group	
hkl	$0kl$	$h0l$	$hk0$	$h00$	$0k0$	$00l$	Extinction symbol	222	$mm2$ $m2m$ $2mm$	mmm
									$I2mm$ (44)	
$h+k+l$	$k+l$	$h+l$	h,k	h	k	l	$I--(ab)$		$Im2a$ (46)	$Imma$ (74)
									$I2mb$ (46)	$Immb$ (74)
$h+k+l$	$k+l$	h,l	$h+k$	h	k	l	$I-(ac)-$		**$Ima2$** (46)	$Imam$ (74)
									$I2cm$ (46)	$Imcm$ (74)
$h+k+l$	$k+l$	h,l	h,k	h	k	l	$I-cb$		$I2cb$ (45)	$Imcb$ (72)
$h+k+l$	k,l	$h+l$	$h+k$	h	k	l	$I(bc)--$		$Iem2$ (46)	$Iemm$ (74)
									$Ie2m$ (46)	
$h+k+l$	k,l	$h+l$	h,k	h	k	l	$Ic-a$		$Ic2a$ (45)	$Icma$ (72)
$h+k+l$	k,l	h,l	$h+k$	h	k	l	$Iba-$		**$Iba2$** (45)	**$Ibam$** (72)
$h+k+l$	k,l	h,l	h,k	h	k	l	$Ibca$			**$Ibca$** (73)
										$Icab$ (73)
$h+k,h+l,k+l$	k,l	h,l	h,k	h	k	l	$F---$	**$F222$** (22)	**$Fmm2$** (42)	$Fmmm$ (69)
									$Fm2m$ (42)	
									$F2mm$ (42)	
$h+k,h+l,k+l$	k,l	$h+l=4n; h,l$	$h+k=4n; h,k$	$h=4n$	$k=4n$	$l=4n$	$F-dd$		$F2dd$ (43)	
$h+k,h+l,k+l$	$k+l=4n; k,l$	h,l	$h+k=4n; h,k$	$h=4n$	$k=4n$	$l=4n$	$Fd-d$		$Fd2d$ (43)	
$h+k,h+l,k+l$	$k+l=4n; k,l$	$h+l=4n; h,l$	h,k		$k=4n$	$l=4n$	$Fdd-$		**$Fdd2$** (43)	
$h+k,h+l,k+l$	$k+l=4n; k,l$	$h+l=4n; h,l$	$h+k=4n; h,k$	$h=4n$	$k=4n$	$l=4n$	$Fddd$			**$Fddd$** (70)

* Pair of space groups with common point group and symmetry elements but differing in the relative location of these elements.

3.1. SPACE-GROUP DETERMINATION AND DIFFRACTION SYMBOLS

Table 3.1.4.1. Reflection conditions, diffraction symbols and possible space groups (cont.)

TETRAGONAL, Laue classes 4/m and 4/mmm (*cont.*)

								Laue class						
								4/m			4/mmm (4/m 2/m 2/m)			
		Reflection conditions						Point group						
hkl	$hk0$	$0kl$	hhl	$00l$	$0k0$	$hh0$	Extinction symbol	4	$\bar{4}$	$4/m$	422	$4mm$	$\bar{4}2m$ $\bar{4}m2$	$4/mmm$
	$h+k$	k			k		$Pnb-$							$P4/nbm$ (125)
	$h+k$	k	l	l	k		$Pnbc$							$P4_2/nbc$ (133)
	$h+k$	l		l	k		$Pnc-$							$P4_2/ncm$ (138)
	$h+k$	l	l	l	k		$Pncc$							$P4/ncc$ (130)
	$h+k$	$k+l$		l	k		$Pnn-$							$P4_2/nnm$ (134)
	$h+k$	$k+l$	l	l	k		$Pnnc$							$P4/nnc$ (126)
$h+k+l$	$h+k$	$k+l$	l	l	k		$I---$	$I4$ (79)	$I\bar{4}$ (82)	$I4/m$ (87)	$I422$ (97)	$I4mm$ (107)	$I\bar{4}2m$ (121)	$I4/mmm$ (139)
													$I\bar{4}m2$ (119)	
$h+k+l$	$h+k$	$k+l$	l	$l=4n$	k		$I4_1--$	$I4_1$ (80)			$I4_122$ (98)			
$h+k+l$	$h+k$	$k+l$	‡	$l=4n$	k	h	$I--d$					$I4_1md$ (109)	$I\bar{4}2d$ (122)	
$h+k+l$	$h+k$	k,l	l	l	k		$I-c-$					$I4cm$ (108)	$I\bar{4}c2$ (120)	$I4/mcm$ (140)
$h+k+l$	$h+k$	k,l	‡	$l=4n$	k	h	$I-cd$					$I4_1cd$ (110)		
$h+k+l$	h,k	$k+l$	l	$l=4n$	k		$I4_1/a--$			$I4_1/a$ (88)				
$h+k+l$	h,k	$k+l$	‡	$l=4n$	k	h	$Ia-d$							$I4_1/amd$ (141)
$h+k+l$	h,k	k,l	‡	$l=4n$	k	h	$Iacd$							$I4_1/acd$ (142)

† Pair of enantiomorphic space groups, *cf.* Section 3.1.5.
‡ Condition: $2h+l=4n; l$.

$I4/mmm$ D_{4h}^{17} $4/mmm$ Tetragonal

No. 139 $I\,4/m\,2/m\,2/m$ Patterson symmetry $I4/mmm$
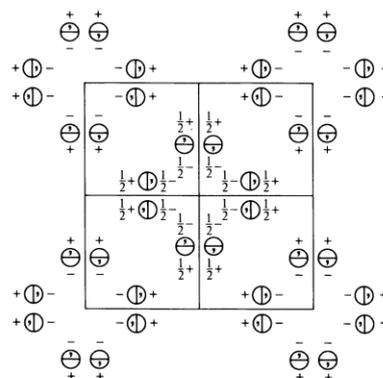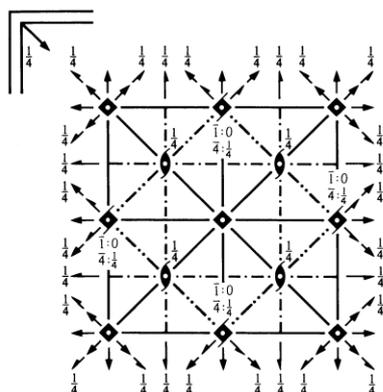
Origin at centre $(4/mmm)$

Asymmetric unit $0 \le x \le \frac{1}{2}; \quad 0 \le y \le \frac{1}{2}; \quad 0 \le z \le \frac{1}{4}; \quad x \le y$

Symmetry operations

For $(0,0,0)+$ set

(1) 1	(2) 2 $0,0,z$	(3) 4^+ $0,0,z$	(4) 4^- $0,0,z$
(5) 2 $0,y,0$	(6) 2 $x,0,0$	(7) 2 $x,x,0$	(8) 2 $x,\bar{x},0$
(9) $\bar{1}$ $0,0,0$	(10) m $x,y,0$	(11) $\bar{4}^+$ $0,0,z;\ 0,0,0$	(12) $\bar{4}^-$ $0,0,z;\ 0,0,0$
(13) m $x,0,z$	(14) m $0,y,z$	(15) m $x,\bar{x},z$	(16) m x,x,z

For $(\frac{1}{2},\frac{1}{2},\frac{1}{2})+$ set

(1) $t(\frac{1}{2},\frac{1}{2},\frac{1}{2})$	(2) $2(0,0,\frac{1}{2})$ $\frac{1}{4},\frac{1}{4},z$	(3) $4^+(0,0,\frac{1}{2})$ $0,\frac{1}{2},z$	(4) $4^-(0,0,\frac{1}{2})$ $\frac{1}{2},0,z$
(5) $2(0,\frac{1}{2},0)$ $\frac{1}{4},y,\frac{1}{4}$	(6) $2(\frac{1}{2},0,0)$ $x,\frac{1}{4},\frac{1}{4}$	(7) $2(\frac{1}{2},\frac{1}{2},0)$ $x,x,\frac{1}{4}$	(8) 2 $x,\bar{x}+\frac{1}{2},\frac{1}{4}$
(9) $\bar{1}$ $\frac{1}{4},\frac{1}{4},\frac{1}{4}$	(10) $n(\frac{1}{2},\frac{1}{2},0)$ $x,y,\frac{1}{4}$	(11) $\bar{4}^+$ $\frac{1}{2},0,z;\ \frac{1}{2},0,\frac{1}{4}$	(12) $\bar{4}^-$ $0,\frac{1}{2},z;\ 0,\frac{1}{2},\frac{1}{4}$
(13) $n(\frac{1}{2},0,\frac{1}{2})$ $x,\frac{1}{4},z$	(14) $n(0,\frac{1}{2},\frac{1}{2})$ $\frac{1}{4},y,z$	(15) c $x+\frac{1}{2},\bar{x},z$	(16) $n(\frac{1}{2},\frac{1}{2},\frac{1}{2})$ x,x,z

Maximal non-isomorphic subgroups *(continued)*

IIa
[2] $P4_2/nmc$ (137)	1; 2; 7; 8; 11; 12; 13; 14; (3; 4; 5; 6; 9; 10; 15; 16)	$+(\frac{1}{2},\frac{1}{2},\frac{1}{2})$
[2] $P4_2/mnm$ (136)	1; 2; 7; 8; 9; 10; 15; 16; (3; 4; 5; 6; 11; 12; 13; 14)	$+(\frac{1}{2},\frac{1}{2},\frac{1}{2})$
[2] $P4_2/nnm$ (134)	1; 2; 5; 6; 11; 12; 15; 16; (3; 4; 7; 8; 9; 10; 13; 14)	$+(\frac{1}{2},\frac{1}{2},\frac{1}{2})$
[2] $P4_2/mmc$ (131)	1; 2; 5; 6; 9; 10; 13; 14; (3; 4; 7; 8; 11; 12; 15; 16)	$+(\frac{1}{2},\frac{1}{2},\frac{1}{2})$
[2] $P4/nmm$ (129)	1; 2; 3; 4; 13; 14; 15; 16; (5; 6; 7; 8; 9; 10; 11; 12)	$+(\frac{1}{2},\frac{1}{2},\frac{1}{2})$
[2] $P4/mnc$ (128)	1; 2; 3; 4; 9; 10; 11; 12; (5; 6; 7; 8; 13; 14; 15; 16)	$+(\frac{1}{2},\frac{1}{2},\frac{1}{2})$
[2] $P4/nnc$ (126)	1; 2; 3; 4; 5; 6; 7; 8; (9; 10; 11; 12; 13; 14; 15; 16)	$+(\frac{1}{2},\frac{1}{2},\frac{1}{2})$
[2] $P4/mmm$ (123)	1; 2; 3; 4; 5; 6; 7; 8; 9; 10; 11; 12; 13; 14; 15; 16	

IIb none

Maximal isomorphic subgroups of lowest index

IIc [3] $I4/mmm$ ($\mathbf{c}' = 3\mathbf{c}$) (139); [9] $I4/mmm$ ($\mathbf{a}' = 3\mathbf{a}, \mathbf{b}' = 3\mathbf{b}$) (139)

Minimal non-isomorphic supergroups

I [3] $Fm\bar{3}m$ (225); [3] $Im\bar{3}m$ (229)

II [2] $C4/mmm$ ($\mathbf{c}' = \frac{1}{2}\mathbf{c}$) ($P4/mmm$, 123)

CONTINUED   No. 139 $I4/mmm$

Generators selected   (1); $t(1,0,0)$; $t(0,1,0)$; $t(0,0,1)$; $t(\frac{1}{2},\frac{1}{2},\frac{1}{2})$; (2); (3); (5); (9)

Positions

Multiplicity, Wyckoff letter, Site symmetry	Coordinates $(0,0,0)+$ $(\frac{1}{2},\frac{1}{2},\frac{1}{2})+$				Reflection conditions

General:

32 o 1	(1) x,y,z	(2) $\bar{x},\bar{y},z$	(3) $\bar{y},x,z$	(4) $y,\bar{x},z$	hkl : $h+k+l=2n$
	(5) $\bar{x},y,\bar{z}$	(6) $x,\bar{y},\bar{z}$	(7) $y,x,\bar{z}$	(8) $\bar{y},\bar{x},\bar{z}$	$hk0$: $h+k=2n$
	(9) $\bar{x},\bar{y},\bar{z}$	(10) $x,y,\bar{z}$	(11) $y,\bar{x},\bar{z}$	(12) $\bar{y},x,\bar{z}$	$0kl$: $k+l=2n$
	(13) $x,\bar{y},z$	(14) $\bar{x},y,z$	(15) $\bar{y},\bar{x},z$	(16) y,x,z	hhl : $l=2n$
					$00l$: $l=2n$
					$h00$: $h=2n$

Special: as above, plus

16 n $.m.$	$0,y,z$	$0,\bar{y},z$	$\bar{y},0,z$	$y,0,z$	no extra conditions
	$0,y,\bar{z}$	$0,\bar{y},\bar{z}$	$y,0,\bar{z}$	$\bar{y},0,\bar{z}$	
16 m $..m$	x,x,z	$\bar{x},\bar{x},z$	$\bar{x},x,z$	$x,\bar{x},z$	no extra conditions
	$\bar{x},x,\bar{z}$	$x,\bar{x},\bar{z}$	$x,x,\bar{z}$	$\bar{x},\bar{x},\bar{z}$	
16 l $m..$	$x,y,0$	$\bar{x},\bar{y},0$	$\bar{y},x,0$	$y,\bar{x},0$	no extra conditions
	$\bar{x},y,0$	$x,\bar{y},0$	$y,x,0$	$\bar{y},\bar{x},0$	
16 k $..2$	$x,x+\frac{1}{2},\frac{1}{4}$	$\bar{x},\bar{x}+\frac{1}{2},\frac{1}{4}$	$\bar{x}+\frac{1}{2},x,\frac{1}{4}$	$x+\frac{1}{2},\bar{x},\frac{1}{4}$	hkl : $l=2n$
	$\bar{x},\bar{x}+\frac{1}{2},\frac{3}{4}$	$x,x+\frac{1}{2},\frac{3}{4}$	$x+\frac{1}{2},\bar{x},\frac{3}{4}$	$\bar{x}+\frac{1}{2},x,\frac{3}{4}$	
8 j $m2m.$	$x,\frac{1}{2},0$	$\bar{x},\frac{1}{2},0$	$\frac{1}{2},x,0$	$\frac{1}{2},\bar{x},0$	no extra conditions
8 i $m2m.$	$x,0,0$	$\bar{x},0,0$	$0,x,0$	$0,\bar{x},0$	no extra conditions
8 h $m.2m$	$x,x,0$	$\bar{x},\bar{x},0$	$\bar{x},x,0$	$x,\bar{x},0$	no extra conditions
8 g $2mm.$	$0,\frac{1}{2},z$	$\frac{1}{2},0,z$	$0,\frac{1}{2},\bar{z}$	$\frac{1}{2},0,\bar{z}$	hkl : $l=2n$
8 f $..2/m$	$\frac{1}{4},\frac{1}{4},\frac{1}{4}$	$\frac{3}{4},\frac{3}{4},\frac{1}{4}$	$\frac{3}{4},\frac{1}{4},\frac{1}{4}$	$\frac{1}{4},\frac{3}{4},\frac{1}{4}$	hkl : $k,l=2n$
4 e $4mm$	$0,0,z$	$0,0,\bar{z}$			no extra conditions
4 d $\bar{4}m2$	$0,\frac{1}{2},\frac{1}{4}$	$\frac{1}{2},0,\frac{1}{4}$			hkl : $l=2n$
4 c $mmm.$	$0,\frac{1}{2},0$	$\frac{1}{2},0,0$			hkl : $l=2n$
2 b $4/mmm$	$0,0,\frac{1}{2}$				no extra conditions
2 a $4/mmm$	$0,0,0$				no extra conditions

Symmetry of special projections

Along [001] $p4mm$ Along [100] $c2mm$ Along [110] $p2mm$
$\mathbf{a}'=\frac{1}{2}(\mathbf{a}-\mathbf{b})$ $\mathbf{b}'=\frac{1}{2}(\mathbf{a}+\mathbf{b})$ $\mathbf{a}'=\mathbf{b}$ $\mathbf{b}'=\mathbf{c}$ $\mathbf{a}'=\frac{1}{2}(-\mathbf{a}+\mathbf{b})$ $\mathbf{b}'=\frac{1}{2}\mathbf{c}$
Origin at $0,0,z$ Origin at $x,0,0$ Origin at $x,x,0$

Maximal non-isomorphic subgroups

I   [2] $I\bar{4}2m$ (121)   (1; 2; 5; 6; 11; 12; 15; 16)+
     [2] $I\bar{4}m2$ (119)   (1; 2; 7; 8; 11; 12; 13; 14)+
     [2] $I4mm$ (107)   (1; 2; 3; 4; 13; 14; 15; 16)+
     [2] $I422$ (97)   (1; 2; 3; 4; 5; 6; 7; 8)+
     [2] $I4/m11$ ($I4/m$, 87)   (1; 2; 3; 4; 9; 10; 11; 12)+
     [2] $I2/m2/m1$ ($Immm$, 71)   (1; 2; 5; 6; 9; 10; 13; 14)+
     [2] $I2/m12/m$ ($Fmmm$, 69)   (1; 2; 7; 8; 9; 10; 15; 16)+

$Fmmm$ D_{2h}^{23} mmm Orthorhombic

No. 69 $F\ 2/m\ 2/m\ 2/m$ Patterson symmetry $Fmmm$
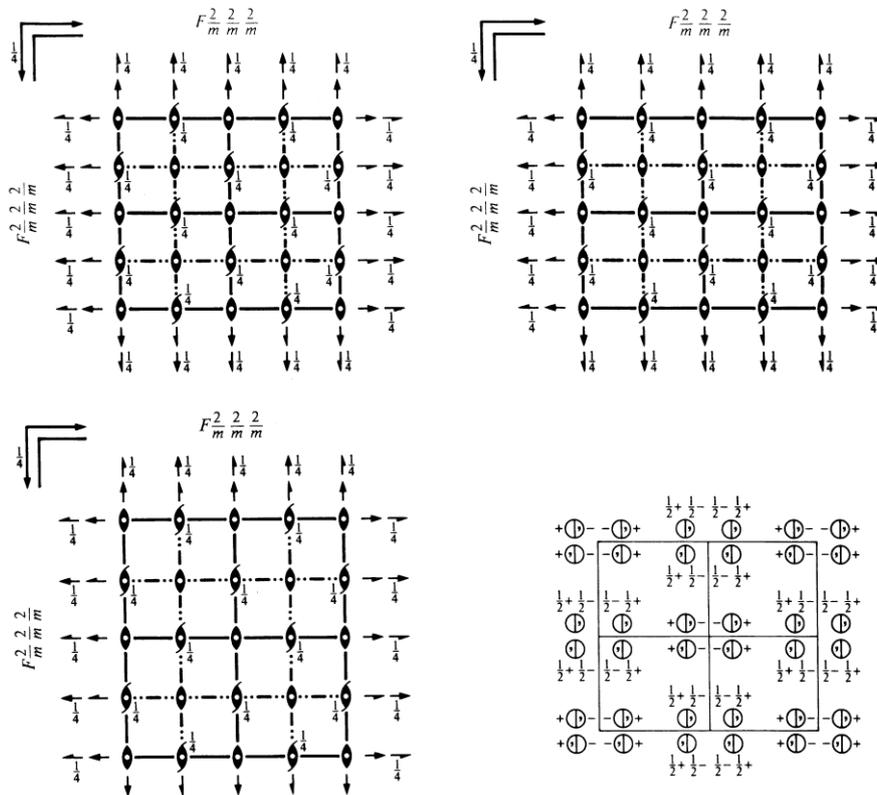
Origin at centre (mmm)

Asymmetric unit $0 \le x \le \frac{1}{4}$; $0 \le y \le \frac{1}{4}$; $0 \le z \le \frac{1}{2}$

Symmetry operations

For $(0,0,0)+$ set

(1) 1	(2) 2 $0,0,z$	(3) 2 $0,y,0$	(4) 2 $x,0,0$
(5) $\bar{1}$ $0,0,0$	(6) m $x,y,0$	(7) m $x,0,z$	(8) m $0,y,z$

For $(0,\frac{1}{2},\frac{1}{2})+$ set

(1) $t(0,\frac{1}{2},\frac{1}{2})$	(2) $2(0,0,\frac{1}{2})$ $0,\frac{1}{4},z$	(3) $2(0,\frac{1}{2},0)$ $0,y,\frac{1}{4}$	(4) 2 $x,\frac{1}{4},\frac{1}{4}$
(5) $\bar{1}$ $0,\frac{1}{4},\frac{1}{4}$	(6) b $x,y,\frac{1}{4}$	(7) c $x,\frac{1}{4},z$	(8) $n(0,\frac{1}{2},\frac{1}{2})$ $0,y,z$

For $(\frac{1}{2},0,\frac{1}{2})+$ set

(1) $t(\frac{1}{2},0,\frac{1}{2})$	(2) $2(0,0,\frac{1}{2})$ $\frac{1}{4},0,z$	(3) 2 $\frac{1}{4},y,\frac{1}{4}$	(4) $2(\frac{1}{2},0,0)$ $x,0,\frac{1}{4}$
(5) $\bar{1}$ $\frac{1}{4},0,\frac{1}{4}$	(6) a $x,y,\frac{1}{4}$	(7) $n(\frac{1}{2},0,\frac{1}{2})$ $x,0,z$	(8) c $\frac{1}{4},y,z$

For $(\frac{1}{2},\frac{1}{2},0)+$ set

(1) $t(\frac{1}{2},\frac{1}{2},0)$	(2) 2 $\frac{1}{4},\frac{1}{4},z$	(3) $2(0,\frac{1}{2},0)$ $\frac{1}{4},y,0$	(4) $2(\frac{1}{2},0,0)$ $x,\frac{1}{4},0$
(5) $\bar{1}$ $\frac{1}{4},\frac{1}{4},0$	(6) $n(\frac{1}{2},\frac{1}{2},0)$ $x,y,0$	(7) a $x,\frac{1}{4},z$	(8) b $\frac{1}{4},y,z$

CONTINUED   No. 69 $F\,mmm$

Generators selected   (1); $t(1,0,0)$; $t(0,1,0)$; $t(0,0,1)$; $t(0,\tfrac{1}{2},\tfrac{1}{2})$; $t(\tfrac{1}{2},0,\tfrac{1}{2})$; (2); (3); (5)

Positions

Multiplicity, Wyckoff letter, Site symmetry	Coordinates $(0,0,0)+$ $(0,\tfrac{1}{2},\tfrac{1}{2})+$ $(\tfrac{1}{2},0,\tfrac{1}{2})+$ $(\tfrac{1}{2},\tfrac{1}{2},0)+$				Reflection conditions
					General:
32 p 1	(1) x,y,z	(2) $\bar{x},\bar{y},z$	(3) $\bar{x},y,\bar{z}$	(4) $x,\bar{y},\bar{z}$	hkl : $h+k,h+l,k+l=2n$
	(5) $\bar{x},\bar{y},\bar{z}$	(6) $x,y,\bar{z}$	(7) $x,\bar{y},z$	(8) $\bar{x},y,z$	$0kl$: $k,l=2n$
					$h0l$: $h,l=2n$
					$hk0$: $h,k=2n$
					$h00$: $h=2n$
					$0k0$: $k=2n$
					$00l$: $l=2n$
					Special: as above, plus
16 o $..m$	$x,y,0$	$\bar{x},\bar{y},0$	$\bar{x},y,0$	$x,\bar{y},0$	no extra conditions
16 n $.m.$	$x,0,z$	$\bar{x},0,z$	$\bar{x},0,\bar{z}$	$x,0,\bar{z}$	no extra conditions
16 m $m..$	$0,y,z$	$0,\bar{y},z$	$0,y,\bar{z}$	$0,\bar{y},\bar{z}$	no extra conditions
16 l $2..$	$x,\tfrac{1}{4},\tfrac{1}{4}$	$\bar{x},\tfrac{3}{4},\tfrac{1}{4}$	$\bar{x},\tfrac{3}{4},\tfrac{3}{4}$	$x,\tfrac{1}{4},\tfrac{3}{4}$	hkl : $h=2n$
16 k $.2.$	$\tfrac{1}{4},y,\tfrac{1}{4}$	$\tfrac{3}{4},\bar{y},\tfrac{1}{4}$	$\tfrac{3}{4},\bar{y},\tfrac{3}{4}$	$\tfrac{1}{4},y,\tfrac{3}{4}$	hkl : $h=2n$
16 j $..2$	$\tfrac{1}{4},\tfrac{1}{4},z$	$\tfrac{3}{4},\tfrac{1}{4},\bar{z}$	$\tfrac{3}{4},\tfrac{3}{4},\bar{z}$	$\tfrac{1}{4},\tfrac{3}{4},z$	hkl : $h=2n$
8 i $mm2$	$0,0,z$	$0,0,\bar{z}$			no extra conditions
8 h $m2m$	$0,y,0$	$0,\bar{y},0$			no extra conditions
8 g $2mm$	$x,0,0$	$\bar{x},0,0$			no extra conditions
8 f 222	$\tfrac{1}{4},\tfrac{1}{4},\tfrac{1}{4}$	$\tfrac{3}{4},\tfrac{3}{4},\tfrac{3}{4}$			hkl : $h=2n$
8 e $..2/m$	$\tfrac{1}{4},\tfrac{1}{4},0$	$\tfrac{3}{4},\tfrac{1}{4},0$			hkl : $h=2n$
8 d $.2/m.$	$\tfrac{1}{4},0,\tfrac{1}{4}$	$\tfrac{3}{4},0,\tfrac{1}{4}$			hkl : $h=2n$
8 c $2/m..$	$0,\tfrac{1}{4},\tfrac{1}{4}$	$0,\tfrac{3}{4},\tfrac{1}{4}$			hkl : $h=2n$
4 b mmm	$0,0,\tfrac{1}{2}$				no extra conditions
4 a mmm	$0,0,0$				no extra conditions

Symmetry of special projections

Along [001] $p\,2mm$ Along [100] $p\,2mm$ Along [010] $p\,2mm$
$\mathbf{a}'=\tfrac{1}{2}\mathbf{a}$ $\mathbf{b}'=\tfrac{1}{2}\mathbf{b}$ $\mathbf{a}'=\tfrac{1}{2}\mathbf{b}$ $\mathbf{b}'=\tfrac{1}{2}\mathbf{c}$ $\mathbf{a}'=\tfrac{1}{2}\mathbf{c}$ $\mathbf{b}'=\tfrac{1}{2}\mathbf{a}$
Origin at $0,0,z$ Origin at $x,0,0$ Origin at $0,y,0$

$Cmce$ D_{2h}^{18} mmm Orthorhombic

No. 64 $C\ 2/m\ 2/c\ 2_1/e$ Patterson symmetry $Cmmm$

Former space-group symbol $Cmca$; *cf.* Chapter 1.3
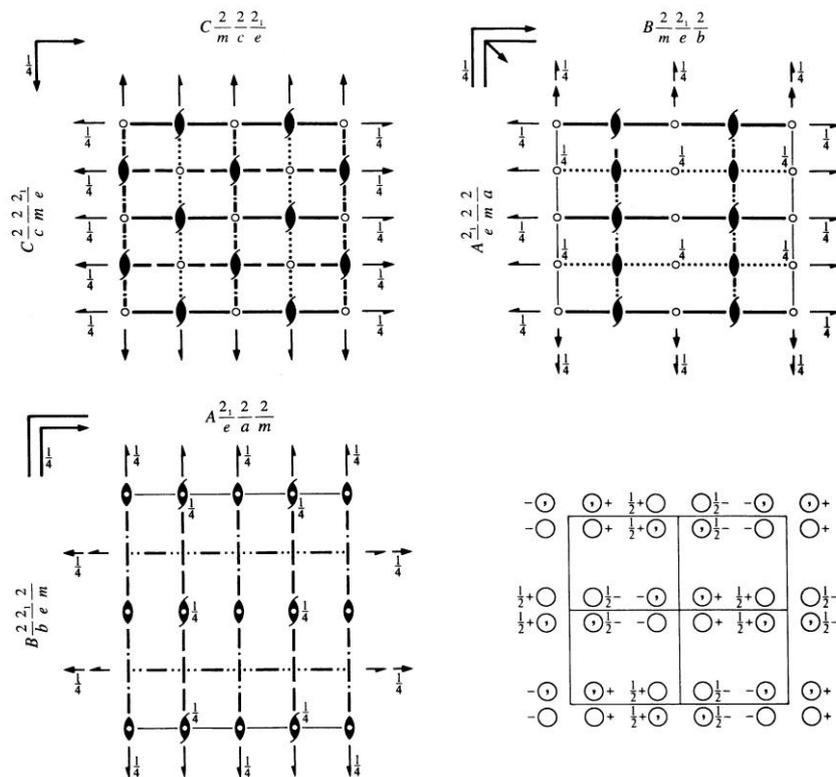
Origin at centre $(2/m)$ at $2/mn\,1$

Asymmetric unit $0 \le x \le \frac{1}{4}$; $0 \le y \le \frac{1}{2}$; $0 \le z \le \frac{1}{2}$

Symmetry operations

For $(0,0,0)+$ set
(1) 1
(2) $2(0,0,\frac{1}{2})$ $0,\frac{1}{4},z$
(3) $2(0,\frac{1}{2},0)$ $0,y,\frac{1}{4}$
(4) 2 $x,0,0$
(5) $\bar{1}$ $0,0,0$
(6) b $x,y,\frac{1}{4}$
(7) c $x,\frac{1}{4},z$
(8) m $0,y,z$

For $(\frac{1}{2},\frac{1}{2},0)+$ set
(1) $t(\frac{1}{2},\frac{1}{2},0)$
(2) $2(0,0,\frac{1}{2})$ $\frac{1}{4},0,z$
(3) 2 $\frac{1}{4},y,\frac{1}{4}$
(4) $2(\frac{1}{2},0,0)$ $x,\frac{1}{4},0$
(5) $\bar{1}$ $\frac{1}{4},\frac{1}{4},0$
(6) a $x,y,\frac{1}{4}$
(7) $n(\frac{1}{2},0,\frac{1}{2})$ $x,0,z$
(8) b $\frac{1}{4},y,z$

CONTINUED   **No. 64**   *C m c e*

Generators selected   (1); $t(1,0,0)$; $t(0,1,0)$; $t(0,0,1)$; $t(\frac{1}{2},\frac{1}{2},0)$; (2); (3); (5)

Positions

Multiplicity, Wyckoff letter, Site symmetry	Coordinates $(0,0,0)+$ $(\frac{1}{2},\frac{1}{2},0)+$				Reflection conditions
16 g 1	(1) x,y,z	(2) $\bar{x},\bar{y}+\frac{1}{2},z+\frac{1}{2}$	(3) $\bar{x},y+\frac{1}{2},\bar{z}+\frac{1}{2}$	(4) $x,\bar{y},\bar{z}$	General:
	(5) $\bar{x},\bar{y},\bar{z}$	(6) $x,y+\frac{1}{2},\bar{z}+\frac{1}{2}$	(7) $x,\bar{y}+\frac{1}{2},z+\frac{1}{2}$	(8) $\bar{x},y,z$	$hkl : h+k=2n$
					$0kl : k=2n$
					$h0l : h,l=2n$
					$hk0 : h,k=2n$
					$h00 : h=2n$
					$0k0 : k=2n$
					$00l : l=2n$
					Special: as above, plus
8 f m..	$0,y,z$	$0,\bar{y}+\frac{1}{2},z+\frac{1}{2}$	$0,y+\frac{1}{2},\bar{z}+\frac{1}{2}$	$0,\bar{y},\bar{z}$	no extra conditions
8 e $.2.$	$\frac{1}{4},y,\frac{1}{4}$	$\frac{3}{4},\bar{y}+\frac{1}{2},\frac{3}{4}$	$\frac{3}{4},\bar{y},\frac{3}{4}$	$\frac{1}{4},y+\frac{1}{2},\frac{1}{4}$	$hkl : h=2n$
8 d $2..$	$x,0,0$	$\bar{x},\frac{1}{2},\frac{1}{2}$	$\bar{x},0,0$	$x,\frac{1}{2},\frac{1}{2}$	$hkl : k+l=2n$
8 c $\bar{1}$	$\frac{1}{4},\frac{1}{4},0$	$\frac{3}{4},\frac{1}{4},\frac{1}{2}$	$\frac{3}{4},\frac{3}{4},\frac{1}{2}$	$\frac{1}{4},\frac{3}{4},0$	$hkl : k,l=2n$
4 b $2/m..$	$\frac{1}{2},0,0$	$\frac{1}{2},\frac{1}{2},\frac{1}{2}$			$hkl : k+l=2n$
4 a $2/m..$	$0,0,0$	$0,\frac{1}{2},\frac{1}{2}$			$hkl : k+l=2n$

Symmetry of special projections

Along $[001]$ $p2mm$	Along $[100]$ $p2gm$	Along $[010]$ $p2mm$
$\mathbf{a}'=\frac{1}{2}\mathbf{a}$ $\mathbf{b}'=\frac{1}{2}\mathbf{b}$	$\mathbf{a}'=\frac{1}{2}\mathbf{b}$ $\mathbf{b}'=\mathbf{c}$	$\mathbf{a}'=\frac{1}{2}\mathbf{c}$ $\mathbf{b}'=\frac{1}{2}\mathbf{a}$
Origin at $0,0,z$	Origin at $x,0,0$	Origin at $0,y,0$

Maximal non-isomorphic subgroups

I   [2] $C2ce$ ($Aea2$, 41)   (1; 4; 6; 7)+
        [2] $Cm2e$ ($Aem2$, 39)   (1; 3; 6; 8)+
        [2] $Cmc2_1$ (36)   (1; 2; 7; 8)+
        [2] $C222_1$ (20)   (1; 2; 3; 4)+
        [2] $C12/c1$ ($C2/c$, 15)   (1; 3; 5; 7)+
        [2] $C112_1/e$ ($P2_1/c$, 14)   (1; 2; 5; 6)+
        [2] $C2/m11$ ($C2/m$, 12)   (1; 4; 5; 8)+

IIa   [2] $Pmnb$ ($Pnma$, 62)   1; 3; 6; 8; (2; 4; 5; 7) + $(\frac{1}{2},\frac{1}{2},0)$
        [2] $Pbca$ (61)   1; 3; 5; 7; (2; 4; 6; 8) + $(\frac{1}{2},\frac{1}{2},0)$
        [2] $Pbna$ ($Pbcn$, 60)   1; 2; 3; 4; (5; 6; 7; 8) + $(\frac{1}{2},\frac{1}{2},0)$
        [2] $Pmca$ ($Pbcm$, 57)   1; 2; 7; 8; (3; 4; 5; 6) + $(\frac{1}{2},\frac{1}{2},0)$
        [2] $Pbnb$ ($Pccn$, 56)   1; 2; 5; 6; (3; 4; 7; 8) + $(\frac{1}{2},\frac{1}{2},0)$
        [2] $Pmcb$ ($Pbam$, 55)   1; 2; 3; 4; 5; 6; 7; 8
        [2] $Pbcb$ ($Pcca$, 54)   1; 4; 6; 7; (2; 3; 5; 8) + $(\frac{1}{2},\frac{1}{2},0)$
        [2] $Pmna$ (53)   1; 4; 5; 8; (2; 3; 6; 7) + $(\frac{1}{2},\frac{1}{2},0)$

IIb   none

Maximal isomorphic subgroups of lowest index

IIc   [3] $Cmce$ ($\mathbf{a}'=3\mathbf{a}$) (64); [3] $Cmce$ ($\mathbf{b}'=3\mathbf{b}$) (64); [3] $Cmce$ ($\mathbf{c}'=3\mathbf{c}$) (64)

Minimal non-isomorphic supergroups

I   none
II   [2] $Fmmm$ (69); [2] $Pmcm$ ($\mathbf{a}'=\frac{1}{2}\mathbf{a},\mathbf{b}'=\frac{1}{2}\mathbf{b}$) ($Pmma$, 51); [2] $Cmme$ ($\mathbf{c}'=\frac{1}{2}\mathbf{c}$) (67)

Contact

HEiDi

Phone: 089/289-14828
Web: http://www.frm2.tum.de/wissenschaftliche-
          nutzung/diffraktion/heidi/index.html

Martin Meven
Institut für Kristallographie Aachen, RWTH Aachen
JCNS Outstation at Forschungsneutronenquelle Heinz Maier-Leibnitz (FRM II)

Phone: 089/289-14727
e-Mail: Martin.Meven@frm2.tum.de